

[REDACTED]

27

N 9 2 - 3 2 5 3 0

A NEW APPROXIMATE FRACTURE MECHANICS ANALYSIS

METHODOLOGY FOR COMPOSITES WITH A CRACK OR HOLE

H. C. Tsai and A. Arocho
Naval Air Development Center

ABSTRACT

A new approximate theory which links the inherent flaw concept with the theory of crack tip stress singularities at a bi-material interface has been developed. Three assumptions were made: (1) the existence of inherent flaw (i.e., damage zone) at the tip of the crack, (2) a fracture of the filamentary composites initiates at a crack lying in the matrix material at the interface of the matrix/filament, (3) the laminate fails whenever the principal load-carrying laminae fails. This third assumption implies that for a laminate consisting of 0° plies, cracks into matrix perpendicular to the 0° filaments are the triggering mechanism for the final failure.

Based on this theory, a parameter \bar{K}_Q which is similar to the stress intensity factor for isotropic materials but with a different dimension was defined. Utilizing existing test data, it was found that \bar{K}_Q can be treated as a material constant. Based on this finding a fracture mechanics analysis methodology was developed.

The analytical results are correlated well with test results. This new approximate theory can apply to both brittle and metal matrix composite laminates with crack or hole.

INTRODUCTION

The failure modes associated with fractures in fiber-reinforced composites differ considerably from those of homogeneous isotropic materials. The failure modes in composites are typically in the forms of transverse cracking, delamination, fiber breaks, matrix yielding, matrix cracking, fiber pull-out and fiber/matrix debonding. As a result, it is very difficult to predict the fracture behavior of composite materials exactly.

In the past, a great deal of effort has been expended to investigate the fracture behavior of composites. A number of fracture mechanics theories have been proposed. These theories have been reviewed and presented extensively in References 1 and 2.

* In this paper a microscopic theory which was originally proposed by Mar and Lin⁹ has been modified into a new theory. This new theory links the inherent flaw concept³⁻⁸, which postulates that a damage zone exists at the tip of crack, with the theory of crack singularities at a bi-material interface⁹⁻¹². This combined theory can be used to predict the notched strength of organic and metal matrix composites with either a crack or a hole.

*This paper cites references 1-20.

THEORY

The stress distribution at the crack tip in a thin plate for a homogeneous, isotropic elastic solid in terms of the coordinates shown in Figure 1 is given by equation (1)

$$\begin{aligned}\sigma_x &= \sigma_N \left(\frac{a_0}{2r}\right)^{1/2} \left[\cos\frac{\theta}{2} \left(1 - \sin\frac{\theta}{2} \sin\frac{3\theta}{2}\right) \right] \\ \sigma_y &= \sigma_N \left(\frac{a_0}{2r}\right)^{1/2} \left[\cos\frac{\theta}{2} \left(1 + \sin\frac{\theta}{2} \sin\frac{3\theta}{2}\right) \right] \\ \tau_{xy} &= \sigma_N \left(\frac{a_0}{2r}\right)^{1/2} \left[\sin\frac{\theta}{2} \cos\frac{\theta}{2} \cos\frac{3\theta}{2} \right]\end{aligned}\tag{1}$$

where

σ_N = gross nominal stress

For an orientation directly ahead of the crack ($\theta = 0$)

$$\sigma_x = \sigma_y = \sigma_N \left(\frac{a_0}{2r}\right)^{1/2} \quad \text{and} \quad \tau_{xy} = 0\tag{2}$$

Irwin¹³ pointed out that equation (1) indicates that the local stresses near a crack depend on the product of the nominal stress and the square root of the half-flaw length. He called this relationship the stress intensity factor K , where for a sharp elastic crack in an infinitely wide plate, K is defined as

$$K = \sigma_N \sqrt{a_0}\tag{3}$$

In the approach using linear-elastic fracture mechanics (LEFM), K is a material parameter and may be determined from tests.

For a finite-width plate, equation (3) is modified to

$$K = Y \sigma_N \sqrt{a_0}\tag{4}$$

Where Y is a parameter that depends on the plate and crack geometry.

To develop similar concept for composite materials, the assumptions of references 3,9 were adopted in this paper; i.e.:

- . The existence of an inherent flaw (also called a damage zone) at the edge of a hole or at the tip of a crack.
- . Fracture of a filamentary composite initiates at a crack lying in the matrix material at the interface of the matrix/filament.
- . A laminate fails whenever the principal load-carrying laminae fails. This implies that cracks in the matrix perpendicular to the 0° filaments are the triggering mechanism for the final failure.

Based on the above assumptions, the following theories are developed:

Using the same concept of stress intensity factor as is formulated above for isotropic materials, a material parameter similar to K is defined for composite material as

$$\overline{K} = Y \sigma_N (a_0)^m \quad (5)$$

where m is the order of singularity of a crack whose tip is at the interface of two different materials as shown in Figure 2. Calculations for determining m are presented in Reference 18.

Note that \overline{K} has a different dimension from K . (K has a dimension of "stress times length to the $1/2$ power", while \overline{K} has a dimension of "stress times length to the m power".)

Although some composite materials (such as polymeric matrix composites) fail in a brittle manner, a damage zone does develop which is analogous to the plastic zone for ductile materials. Using this concept in conjunction with equation (5) yields:

$$\overline{K} = Y \sigma_N (a_0 + C_0)^m \quad (6)$$

where C_0 is defined as an inherent flaw size. The term inherent flaw size is used since unnotched strength, σ_0 , of a composite laminate is given by equation (6) for the case of vanishing a_0 ,

$$\overline{K} = Y_0 \sigma_0 (C_0)^m \quad (7)$$

where Y_0 is the correction factor for infinite plate.

It should be noted that C_0 does not physically refer to an inherent crack, but a characteristic dimension of damage zone at the tip of a notch or crack prior to ultimate failure.

The question we may ask now is whether \overline{K} and C_0 are material constants. Before we reach a conclusion, certain equations are helpful in answering this question.

Substituting equation (7) into equation (6), and after some manipulations, we obtain the following important equations that will be used to determine parameter \bar{K} , C_0 and notched strength of composite laminates

$$C_0 = \frac{a_0}{\left(\frac{\sigma_0}{\bar{Y}_{\sigma_N}}\right)^{1/m} - 1} \quad (8)$$

$$\bar{K} = a_0^m Y_0 \sigma_0 \left\{ \left(\frac{\bar{Y}_{\sigma_N}}{\sigma_0}\right)^{-1/m} - 1 \right\}^{-m} \quad (9)$$

$$\frac{\sigma_N}{\sigma_0} = \frac{1}{\bar{Y}} \left\{ \frac{C_0}{a_0 + C_0} \right\}^m \quad (10)$$

or

$$\frac{\sigma_N}{\sigma_0} = \frac{1}{\bar{Y}} \frac{1}{\left\{ 1 + \left(\frac{Y_0 \sigma_0}{\bar{K}}\right)^{1/m} a_0 \right\}^m} \quad (11)$$

where

$$\bar{Y} = \frac{Y}{Y_0}$$

In the following sections, \bar{K} will be called the equivalent stress intensity factor for composite materials.

DETERMINATION OF EQUIVALENT STRESS INTENSITY FACTOR, \bar{K} AND INHERENT FLAW SIZE C_0

Reference 8 provides extensive fracture test data of boron/aluminum laminates with various proportions of 0° and $\pm 45^\circ$ plies. Hence, this test data will be used to characterize the fracture behavior of boron/aluminum composite laminates.

EQUIVALENT STRESS INTENSITY FACTOR, \bar{K}

From Reference 18, the order of stress singularity at the boron/aluminum interface, m equals to .347. Substituting $m = .347$ in equation (9), the equivalent stress intensity factor for boron/aluminum composite laminate with center crack can be written as follows:

$$\bar{K} = a_0^{.347} \sigma_0 \left\{ \left(\frac{Y_{GN}}{\sigma_0} \right)^{-2.88} - 1 \right\}^{-.347} \quad (12)$$

Equation (12) is used to characterize the critical equivalent stress intensity factor of boron/aluminum laminates with various layups.

By using the fracture test results from Reference 8, equivalent stress intensity factors were calculated from equation (12) and are tabulated on Tables 1 through 4 for boron/aluminum composite with laminate constructions $[0]_{6T}$, $[0_2/\pm 45]_S$, $[\pm 45/0_2]_S$ and $[0/\pm 45]_S$ respectively. Note the test results shown in Tables 1 to 4 are average test results of Reference 8. As shown in Tables 1 to 4, \bar{K} values seem to be a material property and vary with different laminate orientations. \bar{K} values are also plotted on Figures 3 to 6. \bar{K}_{AVG} is the average value of \bar{K} from all the crack sizes. As shown in the figures, \bar{K}_{AVG} can be approximately treated as a material constant. It has to be pointed out here that \bar{K}_{AVG} was obtained by averaging three different widths of plate. For $w = 101.6\text{mm}$ \bar{K} values are almost the same for different $2a_0/w$ ratios.

The detailed calculations of \bar{K} are shown in Reference 18.

The above tests are for center crack specimens. For other crack types and locations ⁵, the calculated equivalent stress intensity factors are shown on Table 5, and are obtained from Reference 18. It can be seen that \bar{K} for these unidirectional boron/aluminum composites is constant for different crack conditions. The reason for the slightly different \bar{K} as compared to Table 1 is due to a different value of ultimate tensile strength.

INHERENT FLAW SIZE, C_0

Two methods were used to calculate the inherent flaw sizes for a composite laminate with center crack.

Least Square Fit

Equation (8), in which C_0 is a proportional constant, can be rearranged to yield

$$a_0 = C_0 \left\{ \left(\frac{Y\sigma_N}{\sigma_0} \right)^{-2.88} - 1 \right\} \quad (13)$$

By using the fracture test data as shown in Tables 1 to 4, and the least square fit, C_0 for various laminate constructions are determined as shown in Table 6.

Average Equivalent Stress Intensity Method

From Equation (7) we have

$$\bar{K}_{AVG} = \sigma_0 (C_0)^m \quad (14)$$

where $m = .347$ for boron/aluminum.

The inherent flaw size can be derived from equation (14) as follows:

$$C_0 = \left(\frac{\bar{K}_{AVG}}{\sigma_0} \right)^{1/m} \quad (15)$$

In the case of boron/aluminum composite, equation (15) becomes

$$C_0 = \left(\frac{\bar{K}_{AVG}}{\sigma_0} \right)^{2.88} \quad (16)$$

The inherent flaw sizes for various laminate constructions were calculated using this method and were also tabulated on Table 6.

We pointed out earlier that C_0 does not physically refer to an inherent crack, but rather to a characteristic dimension of damage zone at a crack tip, prior to fracture failure. Comparing the dimension of C_0 with respect to the crack size of B/Al specimens as shown in Table 1 to 4, it is clear that C_0 cannot be neglected in the calculations of equivalent stress intensity factor. The significance of C_0 will be further discussed later in this paper.

Equation (7) is used to calculate critical equivalent stress intensity factor based on the C_0 determined from least square fit method. These values are also plotted on Figures 3 to 6 as K_{LSF} . It can be seen from the plots that there is not much difference between K_{LSF} and K_{AVG} except in the plot for the $[0/+45]_S$ laminates, where though there is a greater difference between K_{AVG} and K_{LSF} , K_{AVG} provides a better result. For this reason K_{AVG} will be adopted in this paper and will be denoted as K_Q .

APPLICATIONS

Once the critical equivalent stress intensity factor K_Q is known, the fracture strength of the composite laminates can be obtained from equations (10) and (11).

From equation (11), we have a fracture strength prediction formula as follows:

$$\frac{\sigma_N}{\sigma_0} = \frac{1}{Y} \left\{ 1 + \left(\frac{K_Q}{Y_0 \sigma_0} \right)^{-1/m} a_0 \right\}^{-m} \quad (17)$$

From Equation (17), it can be seen that the larger the term K_Q/σ_0 the lesser the notch sensitivity and so from equation (10), we can conclude that the larger the inherent flaw size (i.e., the damage zone size), C_0 , the lesser the notch sensitivity.

In the following subsections, the theory developed here is used to predict the fracture strength of various composite laminates.

BORON/ALUMINUM (B/AL) COMPOSITE

Notched Strength Prediction

For B/Al composite laminates, $m = .347$ and equation (17) becomes

$$\frac{\sigma_N}{\sigma_0} = \frac{1}{Y} \left\{ 1 + \left(\frac{\bar{K}_Q}{Y_0 \sigma_0} \right)^{-2.88} a_0 \right\}^{-.347}$$

(18)

where for a composite laminate with a center crack, Y is assumed to be the same as that for an isotropic material⁸.

$$Y = \left\{ \sec \left(\frac{\pi a_0}{w} \right) \right\}^{1/2}$$

For convenience, data from Tables 1 to 4 and 6 are summarized on Table 7 to be used for the following analysis. Substituting σ_0 and \bar{K}_Q from Table 7 for different ply conditions into equation (18) values for σ_N/σ_0 can be obtained for various crack sizes and are tabulated on Column 7 of Tables 1 to 4. The error shown on Column 8 is defined as the difference between calculated results and test results divided by test results. The analytical results are also plotted on Figures 7 to 10.

As can be seen, the prediction represents the experimental results reasonably well.

The \bar{K}_Q values obtained from center cracked specimens are also used to calculate the strength of B/Al specimens with center holes. Comparison of the analytical results and test results¹⁴ are shown in Figures 11 to 13. Figure 11 shows excellent correlation between test and calculated results for $[0]_{6T}$ laminates with center holes, while in Figure 12 and 13, the maximum percentage error for analytical results is around 13%. The detailed calculations are in reference 18. This confirms the findings of reference 19 and 20 that the length of discontinuity and not the shape appeared to control the fracture strength.

Notch Sensitivity of Boron/Aluminum (B/Al) Composite Laminate

The σ_N/σ_0 test data in Tables 1 to 4 are plotted on Figures 14 to 16 for composite laminate of various widths to check the notched sensitivity of B/Al composites. It is obvious that $[\pm 45/0_2]_S$ is the most notch-sensitive, while $[0/\pm 45]_S$ is the least sensitive to the notch size. For $2a_0/W \leq .1$ $[0]_{6T}$ is more sensitive to the notch size than $[0_2/\pm 45]_S$. For $2a_0/W \geq .1$, the σ_N/σ_0 vs $2a_0/W$ curve for $[0]_{6T}$ and $[0_2/\pm 45]_S$ laminates are almost identical. The trend mentioned above can be detected by using a parameter¹⁵ defined by the ratio \bar{K}_Q/σ_0 as shown in Table 7. The ranking of various laminate configurations for the \bar{K}_Q/σ_0 index is $[0/\pm 45]_S$, $[0_2/\pm 45]_S$, $[0]_{6T}$ and $[\pm 45/0_2]_S$ in descending order. The relative values of \bar{K}_Q/σ_0 show a similar trend to that of damage zone size, C_0 .

It can be concluded that the larger the ratio \overline{K}_Q/σ_0 (or the damage zone size C_0) the less fracture sensitivity there is to the crack size.

GRAPHITE/EPOXY (Gr/Ep) COMPOSITE

Equation (9) is used to characterize the \overline{K}_Q for Gr/Ep composites⁶. The detailed calculations are shown in reference 18. \overline{K}_Q for various ply orientations is plotted as shown in Figures 17 to 19. It can be seen that \overline{K}_Q for Gr/Ep composites can be treated as a material constant. Table 8 summarizes the characterization results of Gr/Ep composite laminates. For Thornel 300 graphite fibers in Narmco 5208 epoxy resin, $m = .297$.

Notched Strength Prediction and Notch Sensitivity

For Gr/Ep composite with center crack, equation (17) becomes

$$\frac{\sigma_N}{\sigma_0} = \frac{1}{Y} \left\{ 1 + \left(\frac{\overline{K}_Q}{\sigma_0} \right)^{-3.367} a_0 \right\}^{-.297}$$

(19)

Substituting \overline{K}_Q and σ_0 from Table 8, into equation (19), the fracture strengths of graphite/epoxy for various laminate constructions can be obtained and are plotted on Figure 20. The detailed calculations are shown in reference 18. As can be seen from the figure, the correlation between calculated and experimental results is very good.

It can also be seen from Figure 20 that the ratio \overline{K}_Q/σ_0 (or the inherent flaw size) in Table 8 can be used as a notch sensitivity indicator. The $[0/90/^{+}45]_S$ laminate is less notch sensitive than the $[0/^{+}45]_S$ and $[0/^{+}45]_{2S}$ laminates and accordingly it has a larger ratio of \overline{K}_Q/σ_0 (or C_0) than the other two laminates.

COMPARISON OF ANALYTICAL RESULTS BETWEEN ANISOTROPIC AND NEW APPROXIMATE MODELS

Composite materials made by combining two materials with different elastic moduli are by nature anisotropic in the gross sense. The anisotropic model for composite materials is to assume that the composite is a homogeneous, anisotropic solid. For an anisotropic fracture $m = .5$.¹⁷ Applying the inherent flaw concept³ for an anisotropic mode with center crack, we have

$$K_Q = Y\sigma_N(a_0 + C_0^*)^{1/2}$$

(20)

$$K_Q = \sigma_0 (C_0^*)^{1/2} \quad (21)$$

Note that K_Q has dimensions different from that of $\overline{K_Q}$ and C_0^* is the inherent flaw size corresponding to an anisotropic model.

Examining equations (20) and (21), we can derive the following useful equations for an anisotropic model

$$C_0^* = \frac{a_0}{\left(\frac{\sigma_0}{Y_{\sigma_N}}\right)^2 - 1} \quad (22)$$

$$\frac{\sigma_N}{\sigma_0} = \frac{1}{Y} \left(\frac{C_0^*}{a_0 + C_0^*} \right)^{1/2} \quad (23)$$

$$K_Q = \sigma_0 (a_0)^{1/2} \left\{ \left(\frac{Y_{\sigma_N}}{\sigma_0} \right)^{-2.0} - 1 \right\}^{-.5} \quad (24)$$

Equation (22) can be used to obtain C_0^* while equation (23) can be used to predict the fracture strength of composite laminates.

Figures 21 to 24 show the comparison of calculated results between the new approximate and anisotropic models. It is clear that the new approximate model predicts better results than the anisotropic model.

CONCLUSIONS AND RECOMMENDATIONS

CONCLUSIONS

- . The methodology developed here can be used to characterize the fracture toughness of the composite laminates and can be used as a design tool to predict the fracture strength of various composite laminates.
- . The parameter \bar{K}_0 which was called critical equivalent stress intensity factor is defined, and can be treated as a material constant for various composite laminates.
- . The new approximate model provides better results than those of the anisotropic model.
- . The larger the ratio $\frac{\bar{K}_0}{\sigma_0}$ (or the damage zone size, C_0), the higher the damage tolerance.

RECOMMENDATIONS

- . Further verification of the new approximate theory with test results of various composite materials is needed.
- . Apply the theory developed here to predict the fracture strength of composite laminates with various crack angles.
- . Develop a methodology to predict the inherent flaw size at the crack tip before fracture.

REFERENCES

1. Adams, D. F. and Mahishi, J.M. "Delamination Micromechanics Analysis", NASA Report, N85-31237, May 1985.
2. Whitney, J. M., "Fracture Analysis of Laminates", Composites Engineered Materials Handbook, ASM International, Volume 1, 1987.
3. Waddoups, M. G., Eisenmann, J. R. and Kaminski, B.E., "Macroscopic Fracture Mechanics of Advanced Composite Materials", Journal of Composite Material, Vol. 5, 1971, p. 446.
4. Bowie, O. L., "Analysis of an Infinite Plate Containing Radial Cracks Originating from the Boundary of an Internal Circular Hole," Journal of Mathematics and Physics, Vol. 35, 1956, p. 60.
5. Adsit, N. R. and Waszczak, J. P. "Fracture Mechanics Correlation of Boron/Aluminum Coupon Containing Stress Risers", ASTM STP 593, 1975.
6. Morris, D. H. and Hahn, H. T., "Fracture Resistance Characterization of Graphite/Epoxy Composites", Composites Materials: Testing and Design, ASTM, STP 617, pp. 5-17, 1976.
7. Awerbuch, J., and Hahn, H. T., "Crack Tip Damage and Fracture Toughness of Boron/Aluminum Composites," Journal of Composite Materials, Vol. 13, April 1979, pp. 82-107.
8. Poc, C. C. Jr., and Sova, J. A. "Fracture Toughness of Boron/Aluminum Laminates with Various Proportions of 0° and $\pm 45^\circ$ Plies,". NASA TP 17.7, 1980.
9. Mar, J. W. and Lin, K. Y., "Fracture Mechanics Correlation for Tensile Failure of Filamentary Composites with Holes", Journal of Aircraft, Vol. 14, p. 703, 1977.
10. Lin, K. Y. and Mar, J.W., "Finite Element Analysis of Stress Intensity Factors for Cracks at a Bi-Material Interface", International Journal of Fracture , 12, pp. 521-531, 1976.
11. Bogy, D. B., "On the Plane Elastostatic Problem of a Loaded Crack Terminating at a Material Interface" Journal of Applied Mechanics Transaction ASME, 38, Series E., No. 4 pp. 911-918, December 1971.
12. Zak, A. R. and Williams, M. L. "Crack Point Stress Singularities at a Bi-Material Interface". Journal of Applied Mechanics, 30. Transaction of ASME, 85, Series E. pp. 142-143, March 1963.
13. Irwin, G. R. "Analysis of Stresses and Strains Near the End of a Crack Traversing a Plate," Journal of Applied Mechanics, Transactions ASME, Vol. 24, 1957.
14. Johnson, W. S. and Bigelow, C. A., "Experimental and Analytical Investigation of Fracture Process of Boron/Aluminum Laminates Containing Notches", NASA TP 2187, 1983.
15. Mandell, J. F., Wang, Su-Su, McGarry, J. Frederick "The Extension of Crack Tip Damage Zones in Fiber Reinforced Plastic Laminates". Journal of Composite Materials, Vol. 9, July 1975.

16. Nuismer, R. J. and Whitney, J. M. "Uniaxial Failure of Composite Laminates Containing Stress Concentrations," *Fracture Mechanics of Composites*, ASTM STP 593, American Society for Testing and Materials, Philadelphia, pp. 117-142, 1975.
17. Wu, E.M., "Strength and Fracture of Composites", *Fracture and Fatigue, Composite Materials*, Vol. 5, 1974.
18. Tsai, H.C. and Arocho, A., "A New Approximate Fracture Mechanics Analysis Methodology for Composites with Cracks or Holes". Report No. NADC-88118-60, 1988.
19. Goree, J. G. and Dharani, R. "Mathematical Modeling of Damage in Unidirectional Composites", NASA Contractor Report 3453, 1981
20. Mar, J. W. and Lin, K.Y., "Fracture of Boron/Aluminum Composites with Discontinuities", *Journal of Composite Materials*, Vol. 11, Oct. 1977, pp. 405-421.

Table 3. Equivalent Stress Intensity Factor For $[\pm 45/0]_s$ B/AI Composite.

w (mm)	a_0 (mm)	ξ	Y	$\left(\frac{\sigma_N}{\sigma_0}\right)_{TEST}$	R (MPa(mm) ^{.347})	$\left(\frac{\sigma_N}{\sigma_0}\right)$	Error %
19.1	.25	.025	1.001	-	-	-	-
19.1	.65	.068	1.003	-	-	-	-
50.8	1.25	.05	1.001	.619	674.7	.633	2.3
50.8	2.55	.1	1.006	.531	716.6	.517	-2.6
50.8	7.6	.3	1.06	.361	720.8	.349	-3.5
50.8	12.7	.5	1.189	.245	647.7	.262	7.0
101.6	2.55	.05	1.001	.528	707.6	.520	-1.6
101.6	5.1	.1	1.006	.423	703.8	.417	-1.3
101.6	15.25	.3	1.06	.281	706.2	.276	-1.6
101.6	25.4	.5	1.189	.201	673.0	.207	3.1

$$R^{AVG} = 693.8 \text{ MPa(mm)}^{.347}$$

$$\sigma_0 = 910.5 \text{ MPa} , \xi = 2a_0/W$$

$$Y = \sqrt{\sec\left(\frac{\pi}{2} \xi\right)}$$

Table 4. Equivalent Stress Intensity Factor For $[0/\pm 45]_s$ B/AI Composite.

w (mm)	a_0 (mm)	ξ	Y	$\left(\frac{\sigma_N}{\sigma_0}\right)_{TEST}$	R (MPa(mm) ^{.347})	$\left(\frac{\sigma_N}{\sigma_0}\right)$	ERROR %
19.1	.25	.025	1.001	-	-	-	-
19.1	.65	.068	1.003	.828	564.6	.865	4.4
50.8	1.25	.05	1.001	.796	645.8	.789	-1.0
50.8	2.55	.1	1.006	.730	710.1	.688	-5.7
50.8	7.6	.3	1.06	.458	597.8	.481	5.2
50.8	12.7	.5	1.189	.329	563.1	.367	11.5
101.6	2.55	.05	1.001	.699	656.5	.692	-1.0
101.6	5.1	.1	1.006	.620	702.0	.569	-8.2
101.6	15.25	.3	1.06	.413	678.0	.388	-6.0
101.6	25.4	.5	1.189	.271	583.9	.293	8.2

$$R^{AVG} = 633.5 \text{ MPa(mm)}^{.347}$$

$$\sigma_0 = 581.4 \text{ MPa} , \xi = 2a_0/W$$

$$Y = \sqrt{\sec\left(\frac{\pi}{2} \xi\right)}$$

Table 1. Equivalent Stress Intensity Factor For $[0]_6T$ B/Al Composite.

w (mm)	a_0 (mm)	ξ	Y	$\left(\frac{\sigma_N}{\sigma_0}\right)_{TEST}$	R (MPa(mm) ^{.347})	$\left(\frac{\sigma_N}{\sigma_0}\right)$	Error %
19.1	.25	.025	1.001	.818	1125.0	.878	7.4
19.1	.65	.068	1.003	.6845	1136.0	.760	11.0
50.8	1.25	.05	1.001	.592	1166	.663	12.0
50.8	2.55	.1	1.006	.555	1455	.546	-1.6
50.8	7.6	.3	1.06	.4003	1479	.3705	-7.5
50.8	12.7	.5	1.189	.3098	1518	.279	-10.0
101.6	2.55	.05	1.001	.580	1455	.549	-5.3
101.6	5.1	.1	1.006	.468	1435	.443	-5.3
101.6	15.25	.3	1.06	.3024	1399	.295	-2.6
101.6	25.4	.5	1.189	.232	1430	.221	-4.7

$$R^{AVG} = 1360 \text{ MPa (mm)}^{.347}$$

$$\sigma_0 = 1672 \text{ MPa} , \xi = 2a_0/W$$

$$Y = \sqrt{\sec\left(\frac{\pi}{2}\xi\right)}$$

Table 2. Equivalent Stress Intensity Factor For $[0_2/\pm 45]_s$ B/Al Composite.

w (mm)	a_0 (mm)	ξ	Y	$\left(\frac{\sigma_N}{\sigma_0}\right)_{TEST}$	R (MPa(mm) ^{.347})	$\left(\frac{\sigma_N}{\sigma_0}\right)$	Error %
19.1	.25	.025	1.001	.878	652.6	.891	1.5
19.1	.65	.068	1.003	.782	681.9	.782	0.
50.8	1.25	.05	1.001	.721	740.	.686	-4.8
50.8	2.55	.1	1.006	.571	683.1	.570	0.
50.8	7.6	.3	1.06	.395	697.8	.389	-1.5
50.8	12.7	.5	1.189	.274	639.0	.293	7.0
101.6	2.55	.05	1.001	.579	695.1	.572	-1.2
101.6	5.1	.1	1.006	.464	680.6	.464	0.
101.6	15.25	.3	1.06	.321	711.5	.310	-3.5
101.6	25.4	.5	1.189	.229	674.6	.232	1.6

$$R^{AVG} = 685.6 \text{ MPa (mm)}^{.347}$$

$$\sigma_0 = 800.1 \text{ MPa} , \xi = 2a_0/W$$

$$Y = \sqrt{\sec\left(\frac{\pi}{2}\xi\right)}$$

Table 5. Critical Equivalent Stress Intensity Factor Of Unidirectional B/Al⁵ Composite.

SPECIMEN *	$\frac{2a_o}{w}$ or $\frac{2R}{w}$	\bar{K}_{AVG} MPa (mm) ^{-3/2}
CH	.25	1196.00
CS	.40	1227.00
DEN	.30	1214.00

* CH - CENTER HOLE SPECIMEN

CS - CENTER SLIT SPECIMEN

DEN - DOUBLE EDGE NOTCH SPECIMEN

Table 6. Inherent Flaw Size, C_o (mm).

	Least Square Fit	\bar{K}_{AVG} Method
[0] _{6T}	.633	.552
[0 ₂ /±45] _s	.593	.641
[±45/0 ₂] _s	.405	.457
[0/±45] _s	.976	1.28

Table 7. Fracture Parameters For Various Laminate Configurations Of B/Al.

Ply Configuration	σ_0 (MPa)	\bar{K}_Q MPa (mm) ^{.347}	$\frac{\bar{K}_Q}{\sigma_0}$ MPa (mm) ^{.347}	C_0 (mm)
[0] _{6T}	1672	1360	.81	.552
[0 ₂ /±45] _s	800.1	685.6	.867	.641
[±45/0 ₂] _s	910.5	693.8	.762	.457
[0/±45] _s	581.4	633.5	1.09	1.28

Table 8. Fracture Parameters For Various Laminate Configurations Of Gr/Ep.

Ply Configuration	σ_0 (MPa)	\bar{K}_Q MPa (mm) ^{.297}	$\frac{\bar{K}_Q}{\sigma_0}$ (mm) ^{.297}	C_0 (mm)
[0/±45] _{2s}	541.0	408.6	.755	.389
[0/±45] _s	541.0	393.5	.727	.342
[0/90/±45] _s	454.0	437.7	.964	.884

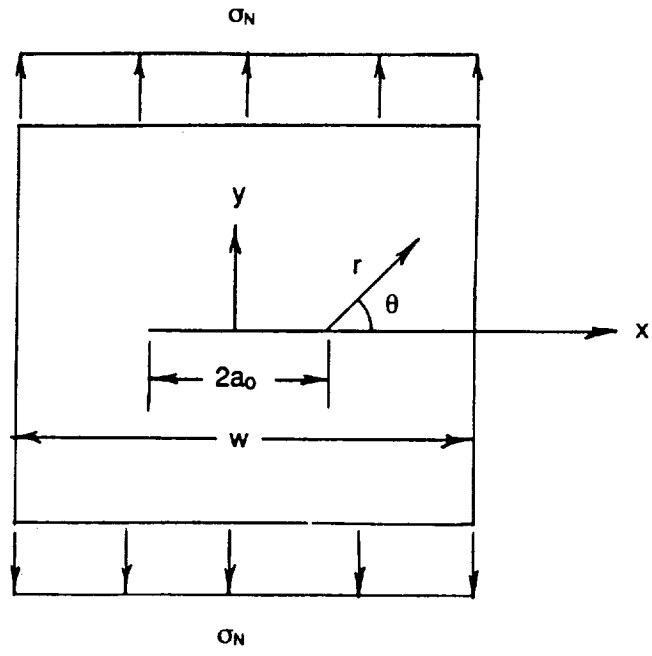


Figure 1. Model For Equations For Stresses At A Point Near A Crack.

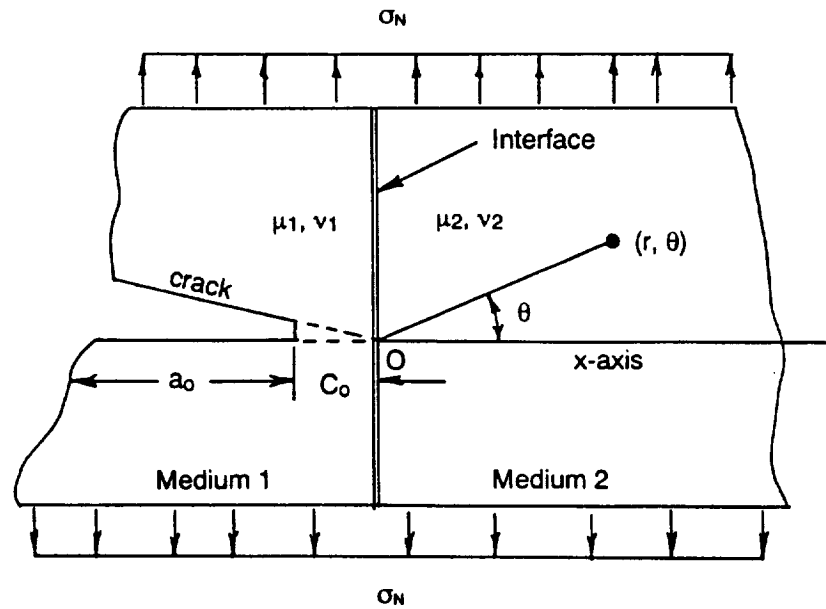


Figure 2. Crack Normal To The Bi-Material Interface With Inherent Flaw, C_0 .

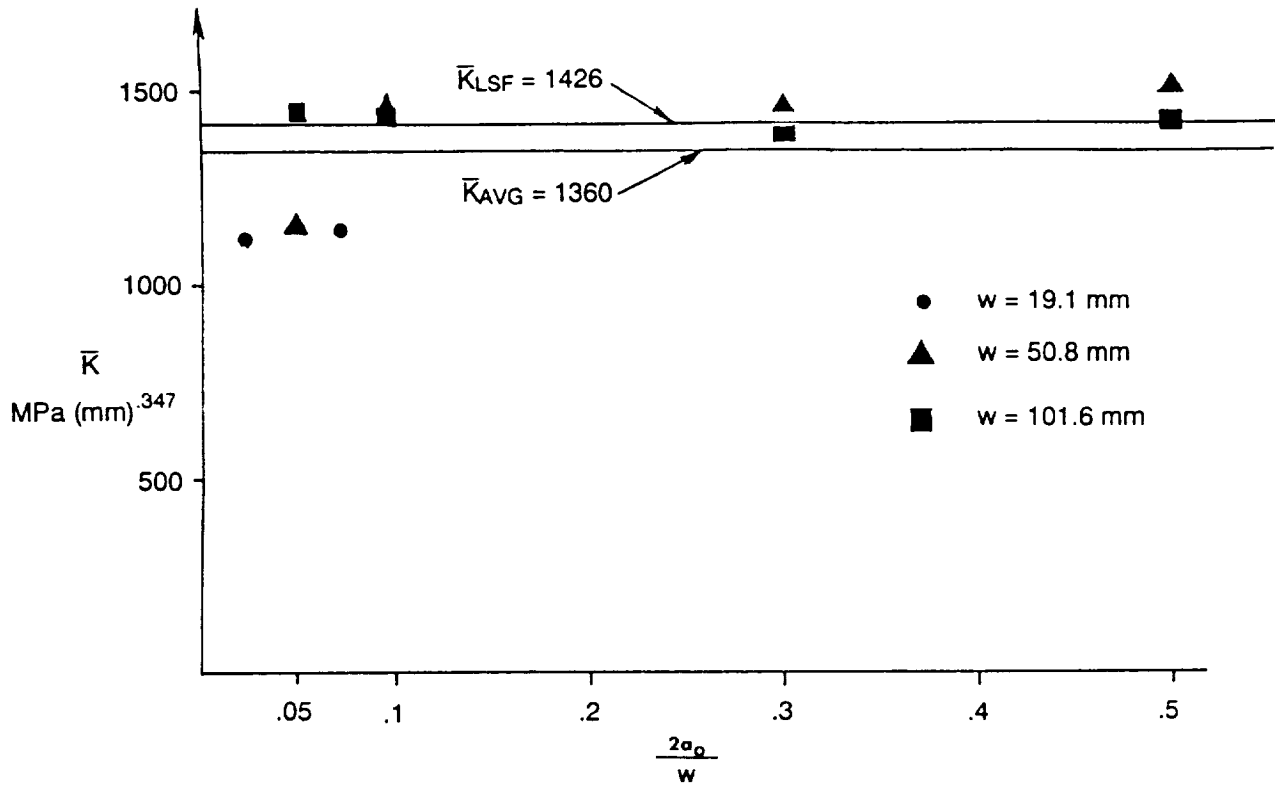


Figure 3. Equivalent Stress Intensity Factor For [0]_{6T} B/Al Composite.

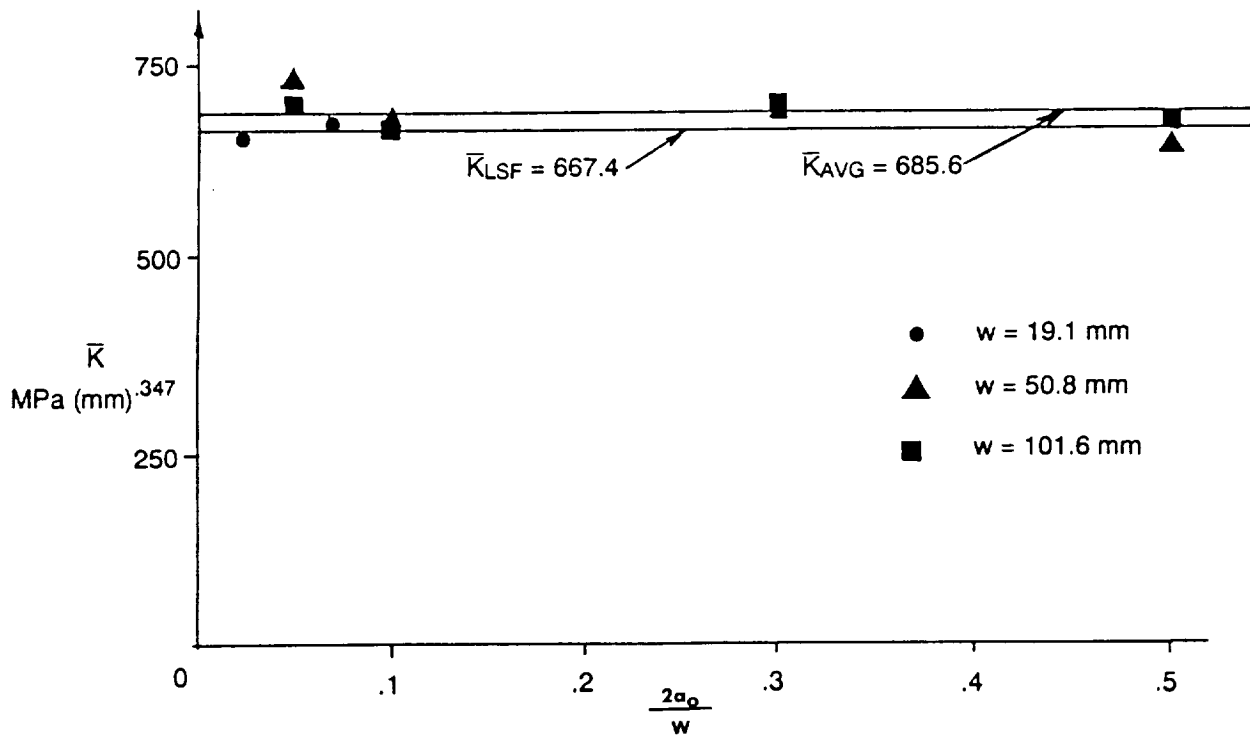


Figure 4. Equivalent Stress Intensity Factor For [0_{2/±45}]_S B/Al Composite.

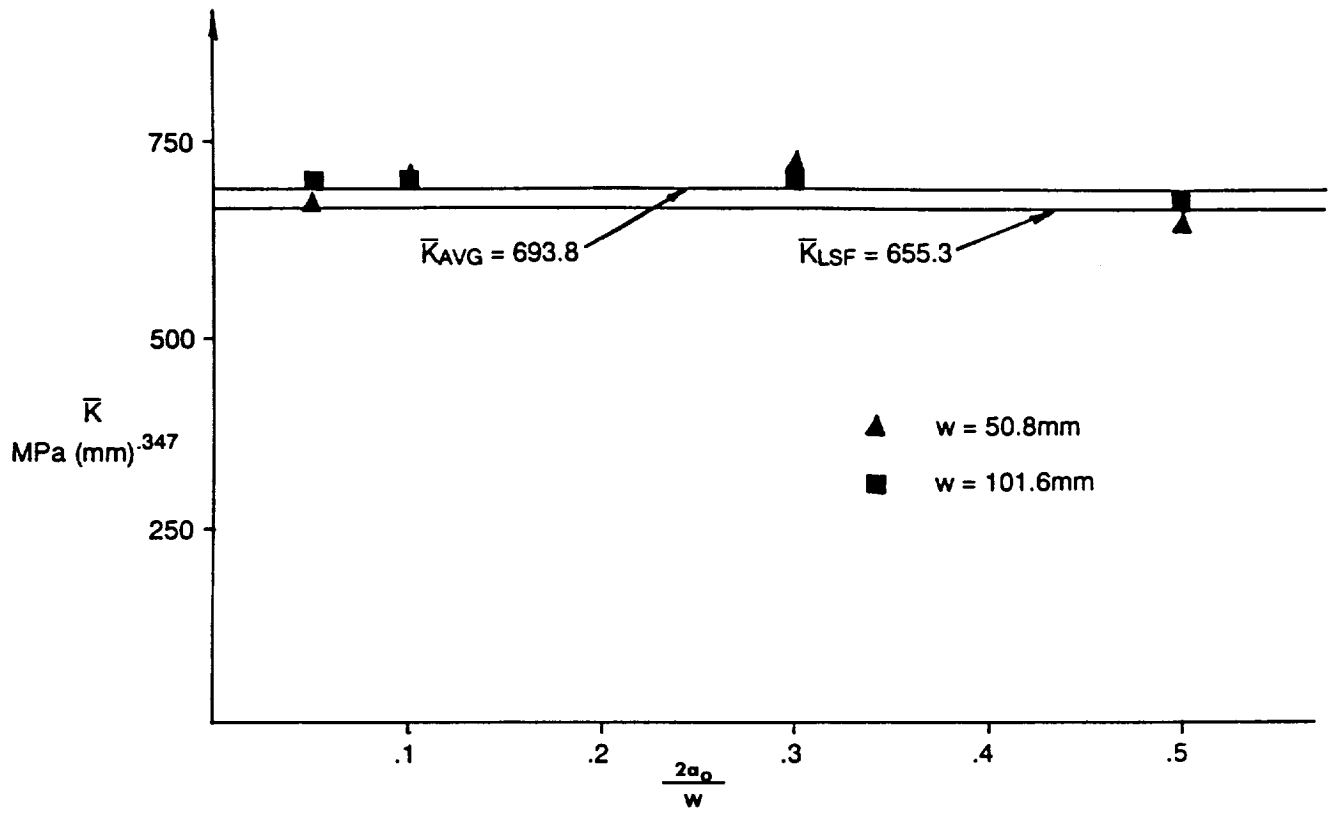


Figure 5. Equivalent Stress Intensity Factor For $[\pm 45/0_2]_s$ B/Al Composite.

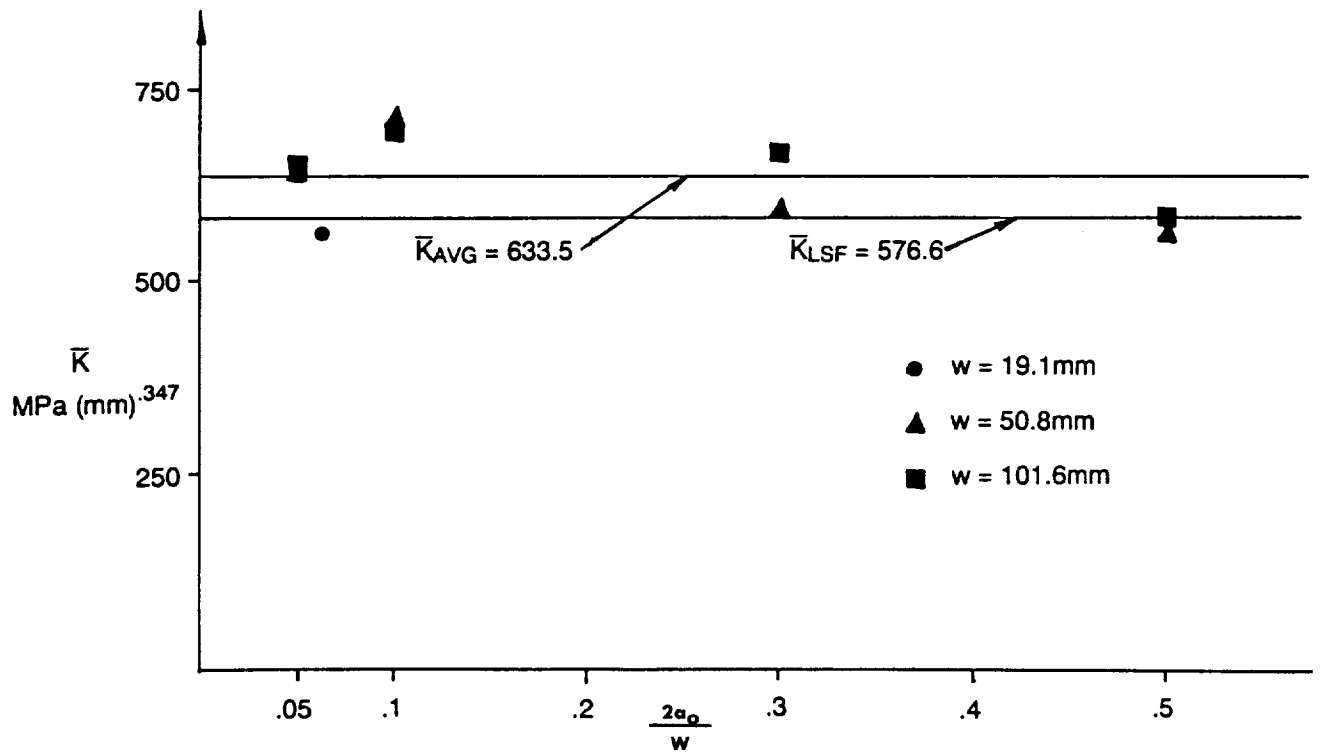


Figure 6. Equivalent Stress Intensity Factor For $[0/\pm 45]_s$ B/Al Composite.

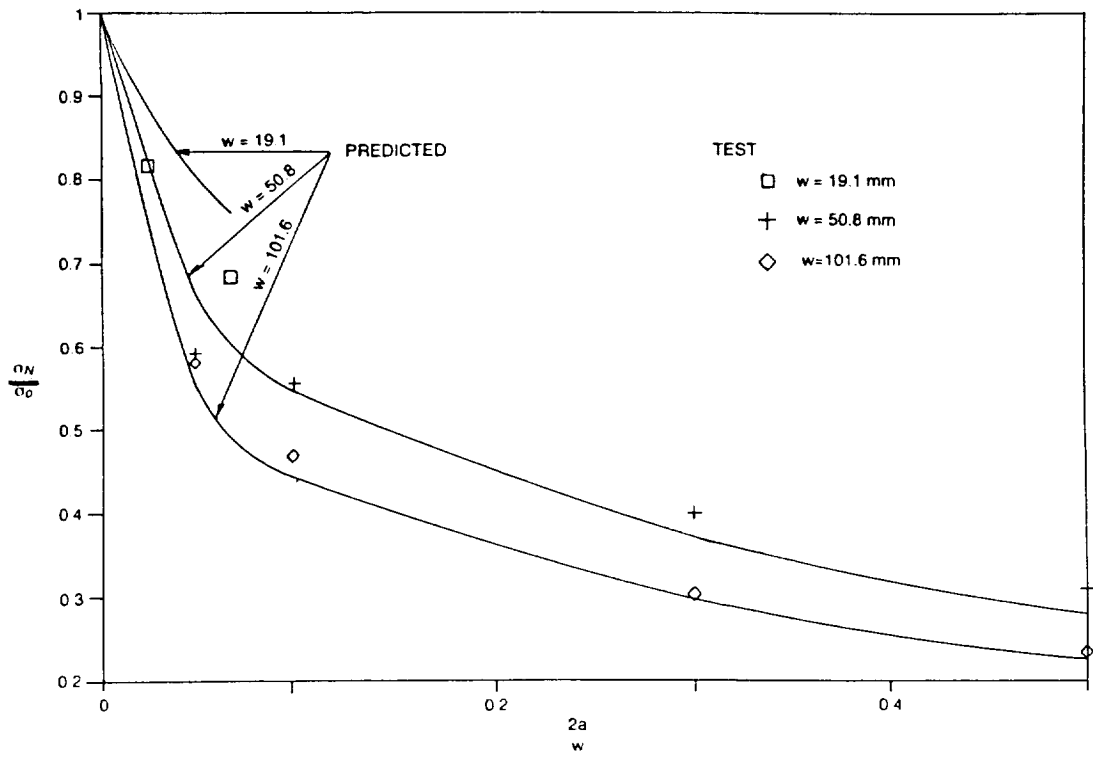


Figure 7 Comparison Of Predicted And Experimental Notched Strength Results For B/AI (0°)6T Composites.

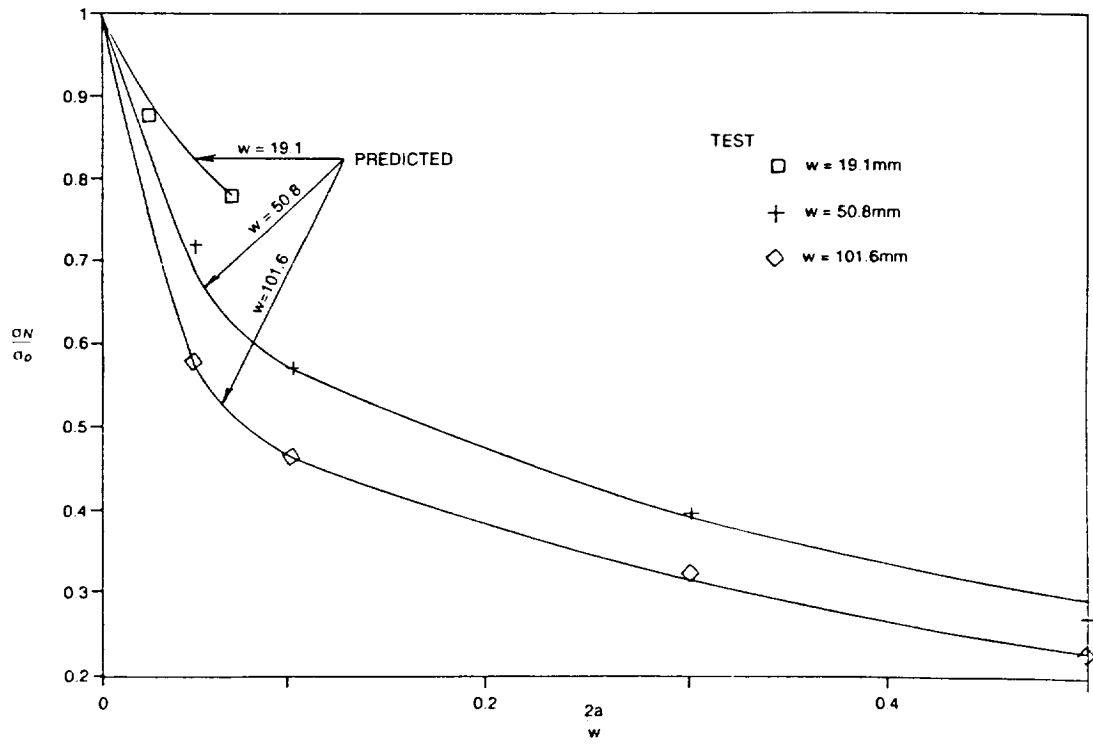


Figure 8. Comparison Of Predicted And Experimental Notched Strength Results For B/AI [02/±45]s Composites.

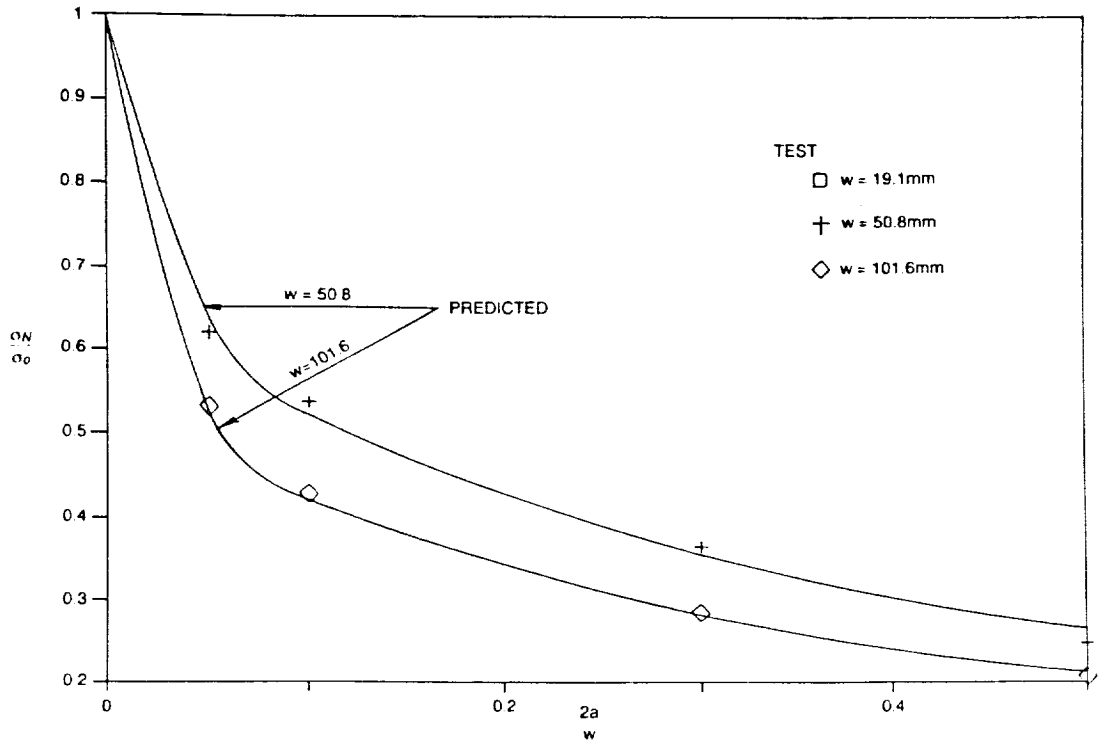


Figure 9 Comparison Of Predicted And Experimental Notched Strength Results For B/AI $[\pm 45/0]_2$ Composites.

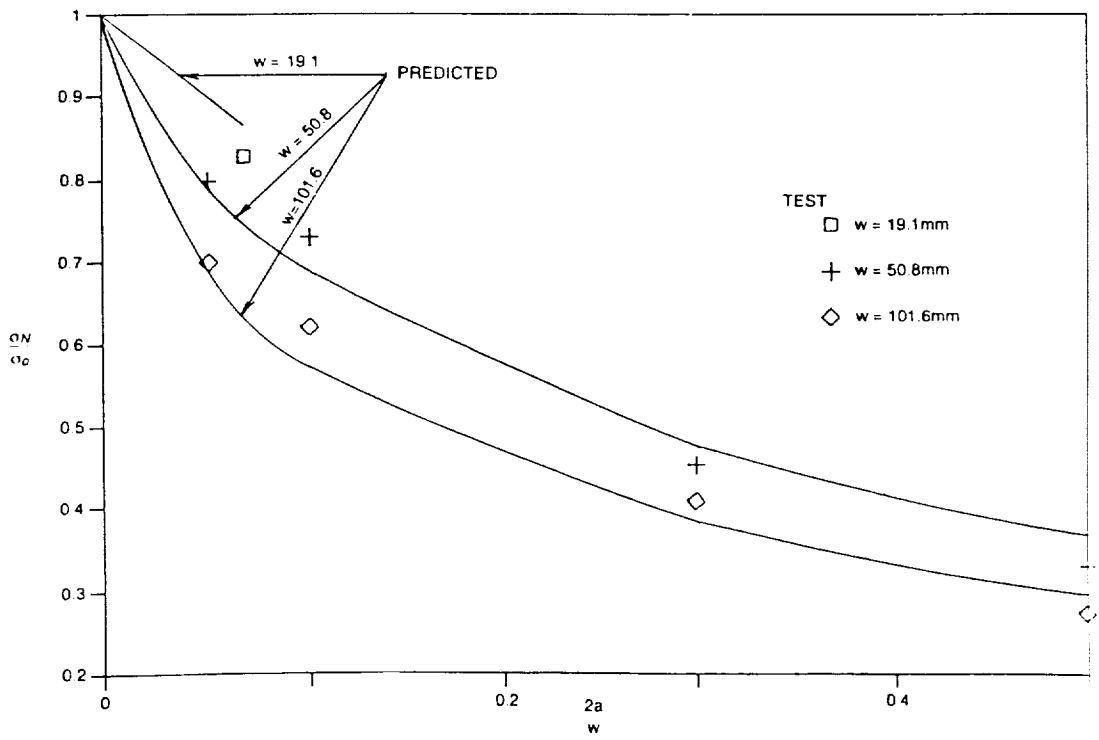


Figure 10 Comparison Of Predicted And Experimental Notched Strength Results For B/AI $[0/\pm 45]_3$ Composites.

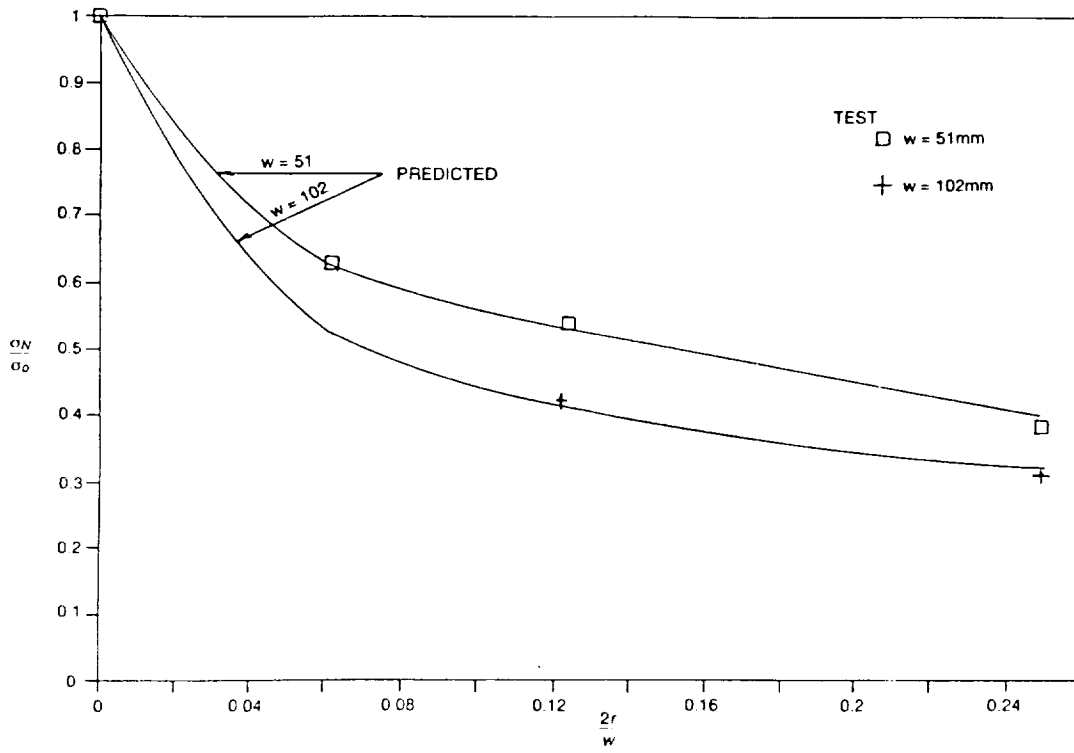


Figure 11. Notched Strength Prediction For B/Al [0]₆T Composite With Center Hole.

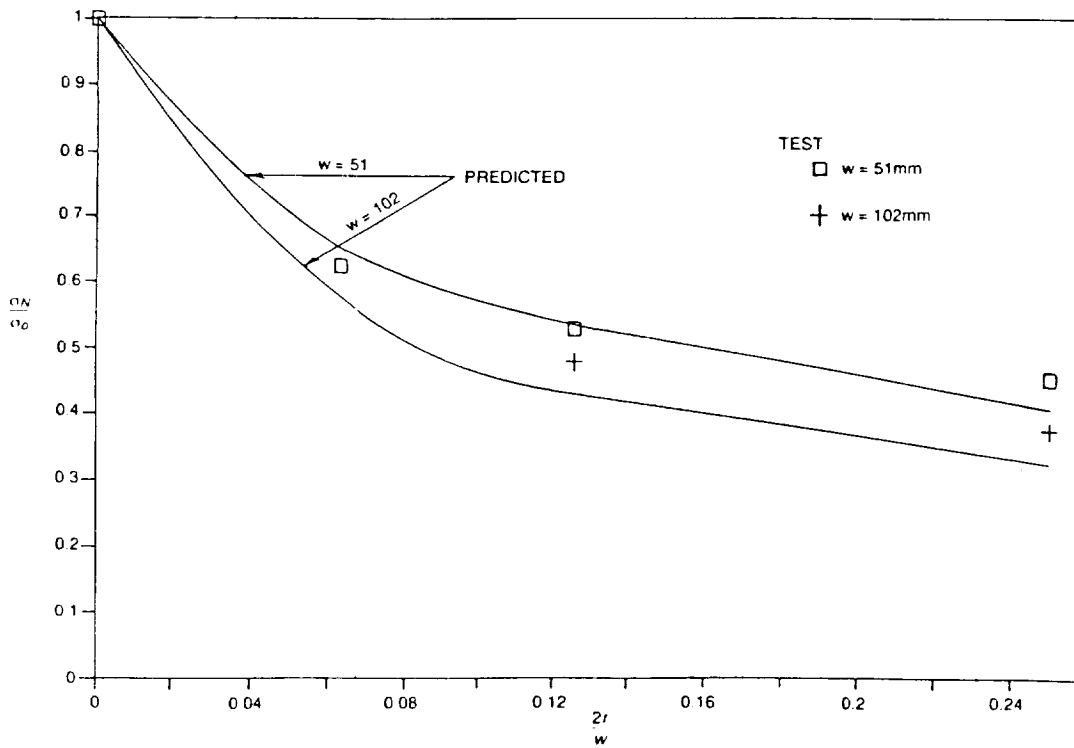


Figure 12. Notched Strength Prediction for B/Al [0₂/z₄₅]_s Composites With Center Hole.

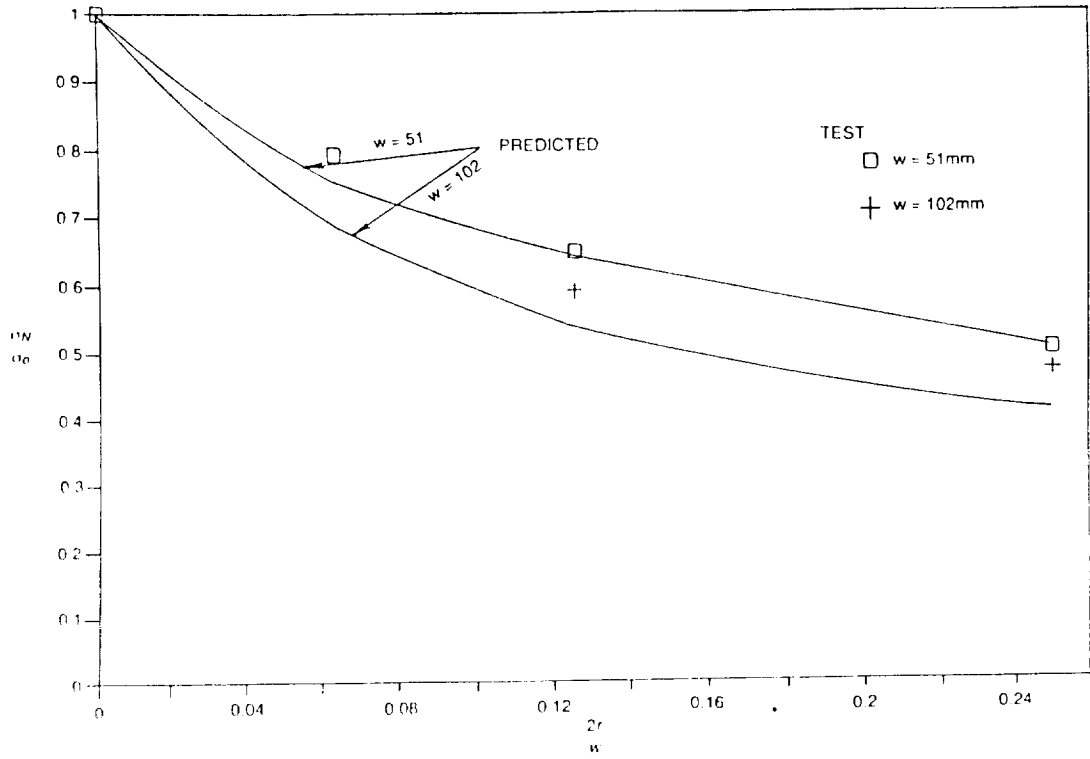


Figure 13 Notched Strength Prediction For B/AI [0/±45]_s Composite With Center Hole.

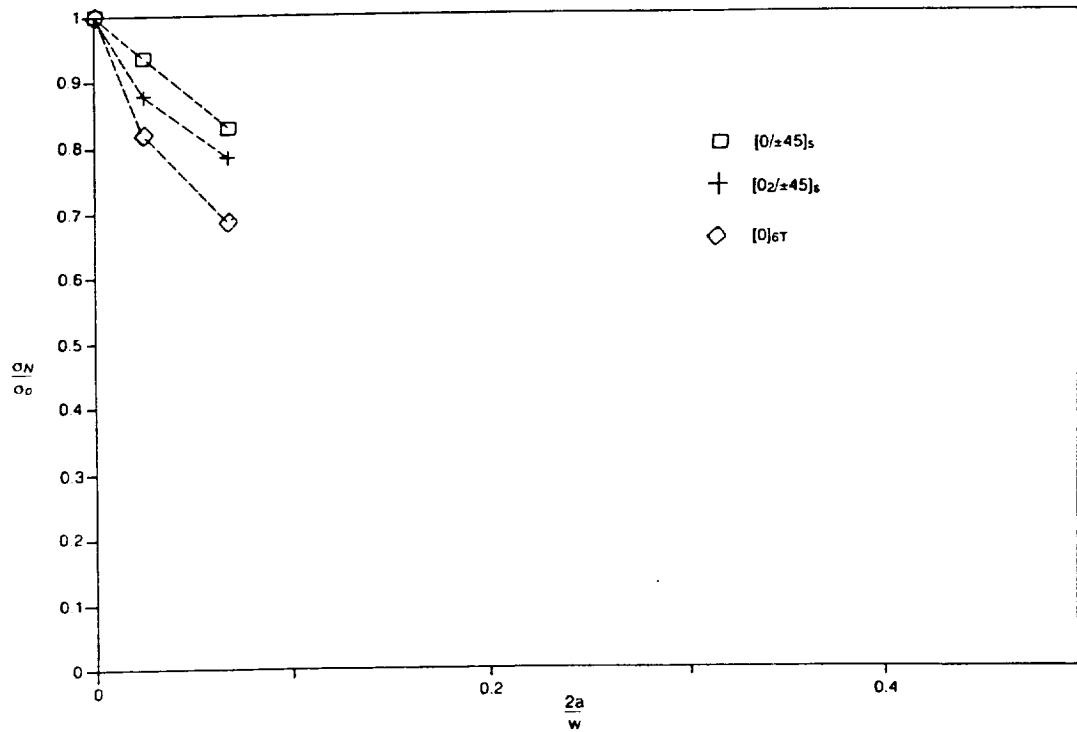


Figure 14. Notch Sensitivities For Various B/AI Laminate Orientations ($w = 19.1\text{mm}$).

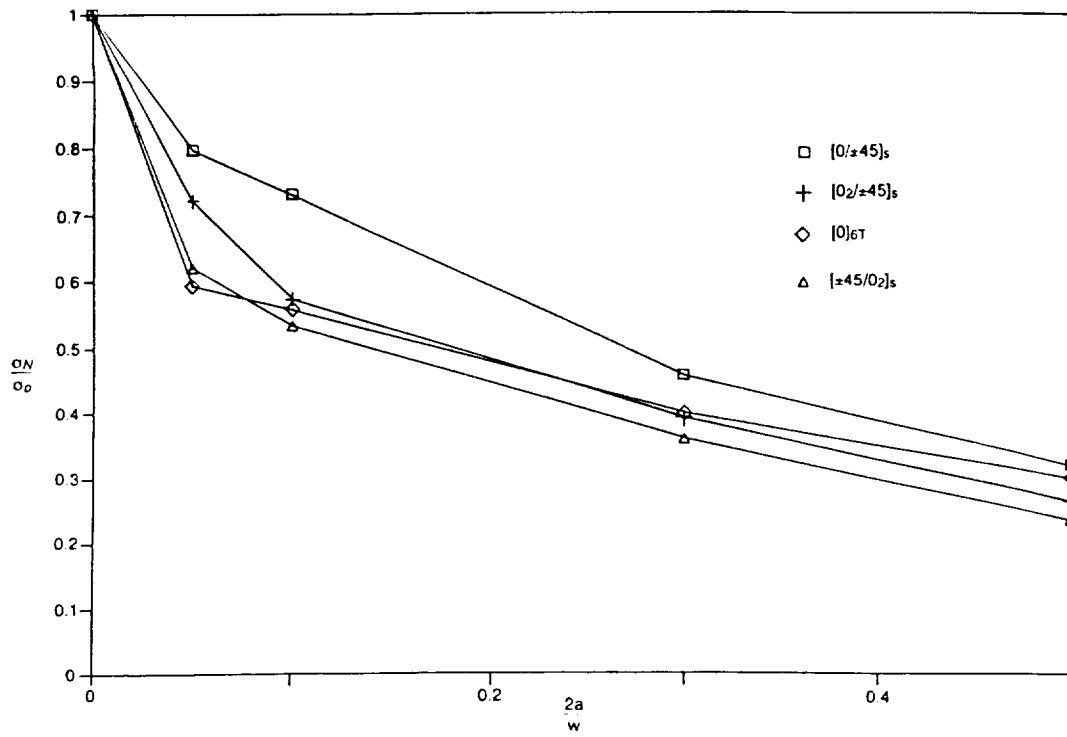


Figure 15. Notch Sensitivities For Various B/AI Laminate Orientations ($w = 50.8\text{mm}$).

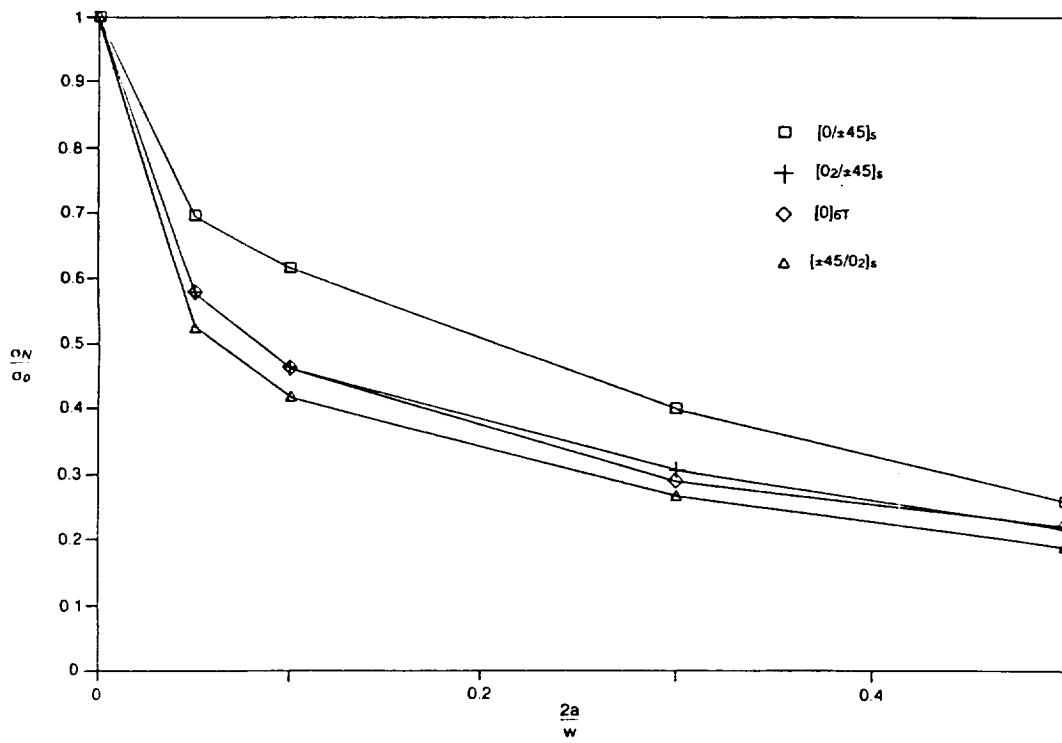


Figure 16. Notch Sensitivities For Various B/AI Laminate Orientations ($w = 101.6\text{mm}$).

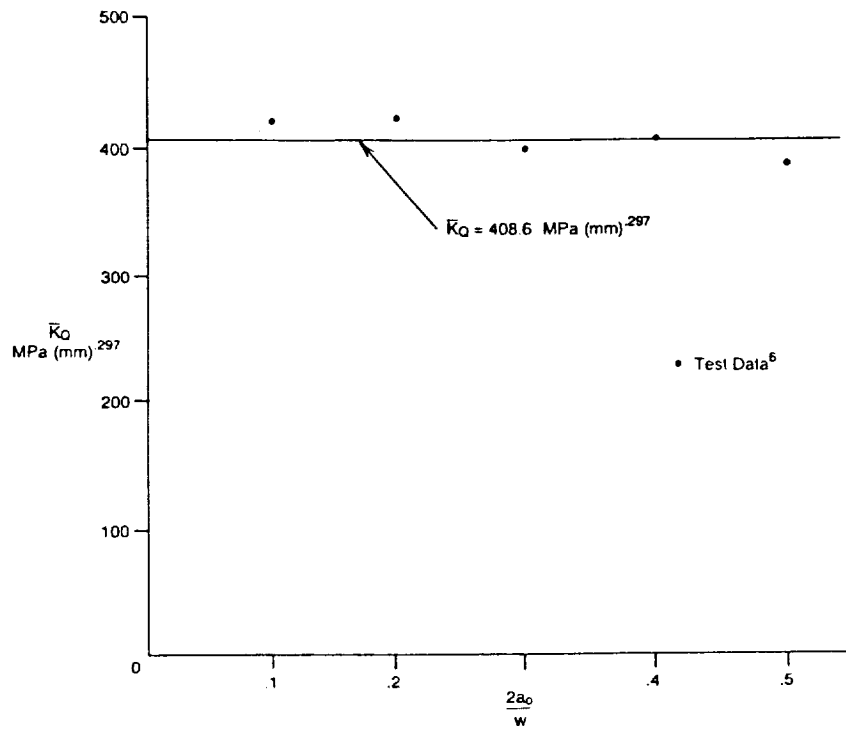


Figure 17. \bar{K}_Q For Gr/Ep With Ply Orientation $[0/\pm 45]_2s$.

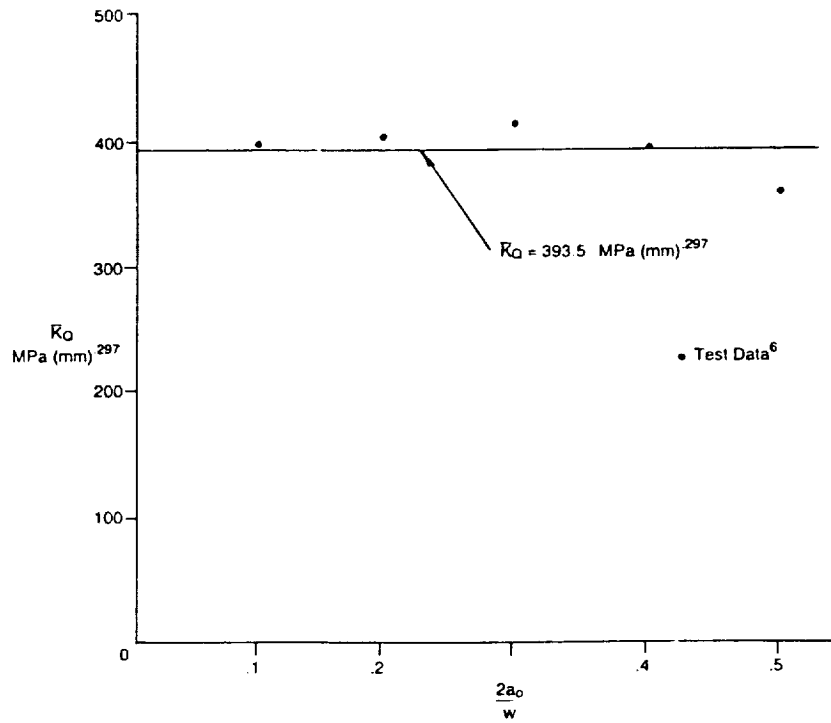


Figure 18 \bar{K}_Q for Gr/Gp With Ply Orientation $[0/\pm 45]_2s$.

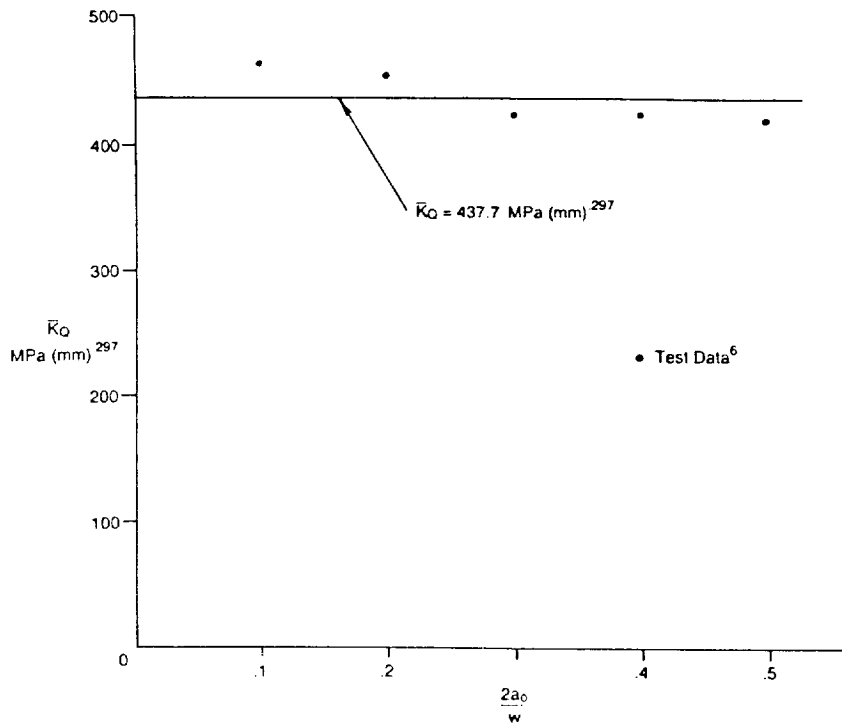


Figure 19. \bar{K}_Q For Gr/Ep With Ply Orientation $[0/90/\pm 45]_s$.

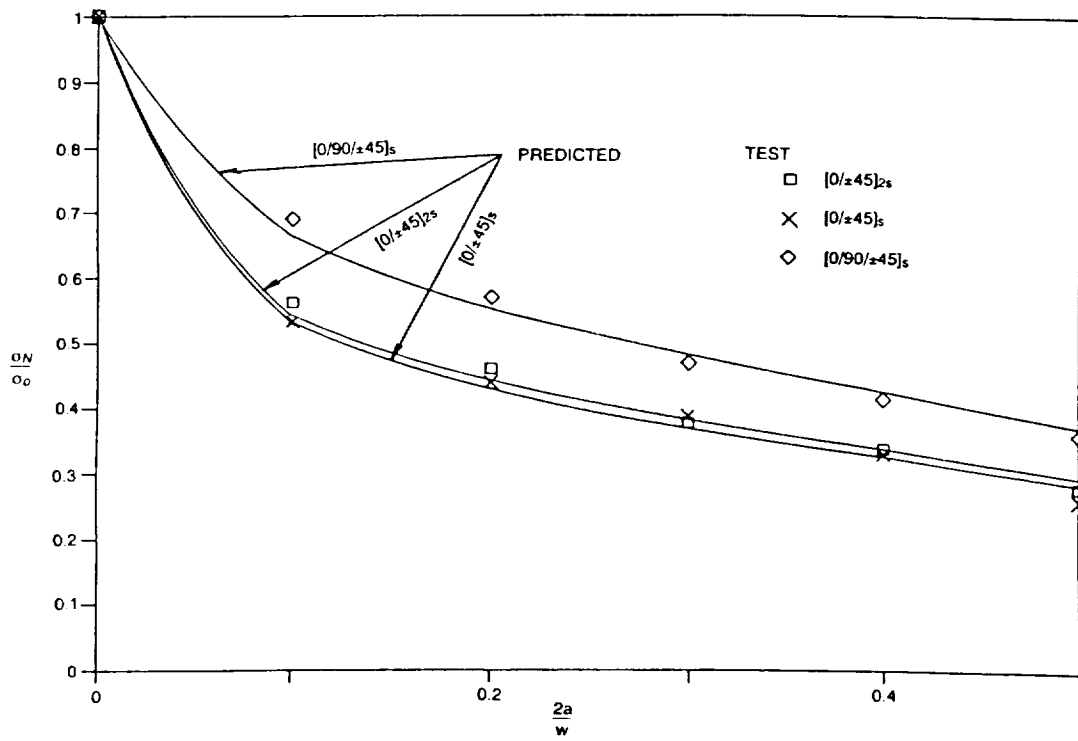


Figure 20. Notch Strength And Notch Sensitivities For Various Gr/Ep Laminate Orientations.

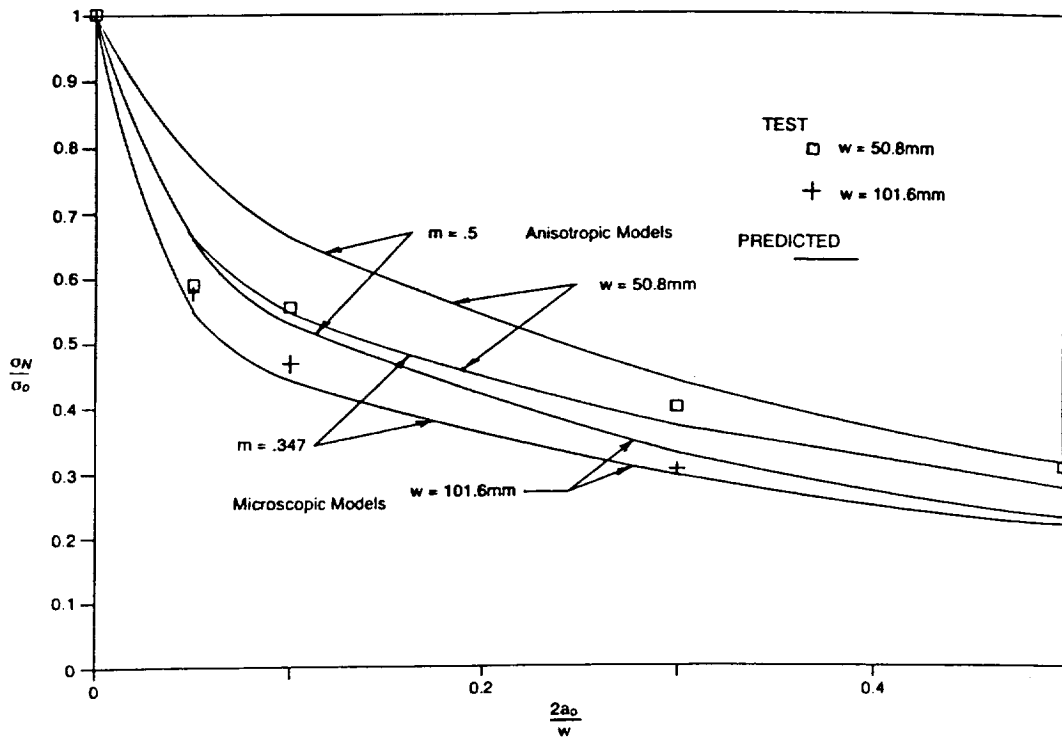


Figure 21. Comparison Of Analytical Results Between Anisotropic And New Approximate Models B/AI (0)6T

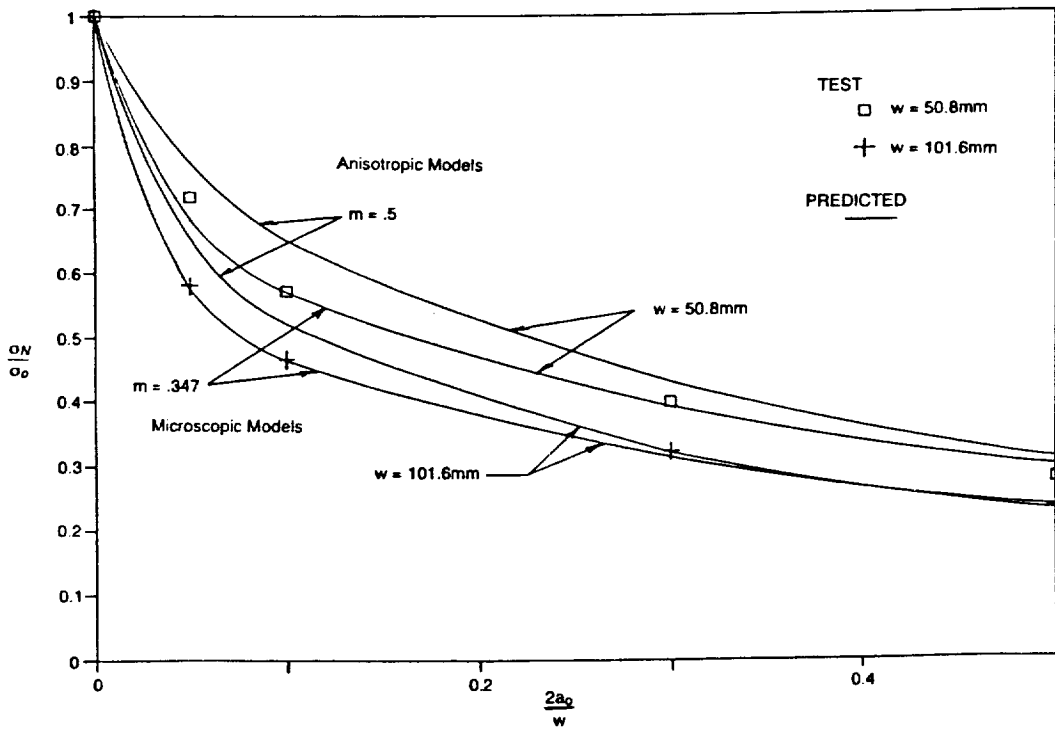


Figure 22. Comparison Of Analytical Results Between Anisotropic And New Approximate Models B/AI (0₂ / ± 45)_s

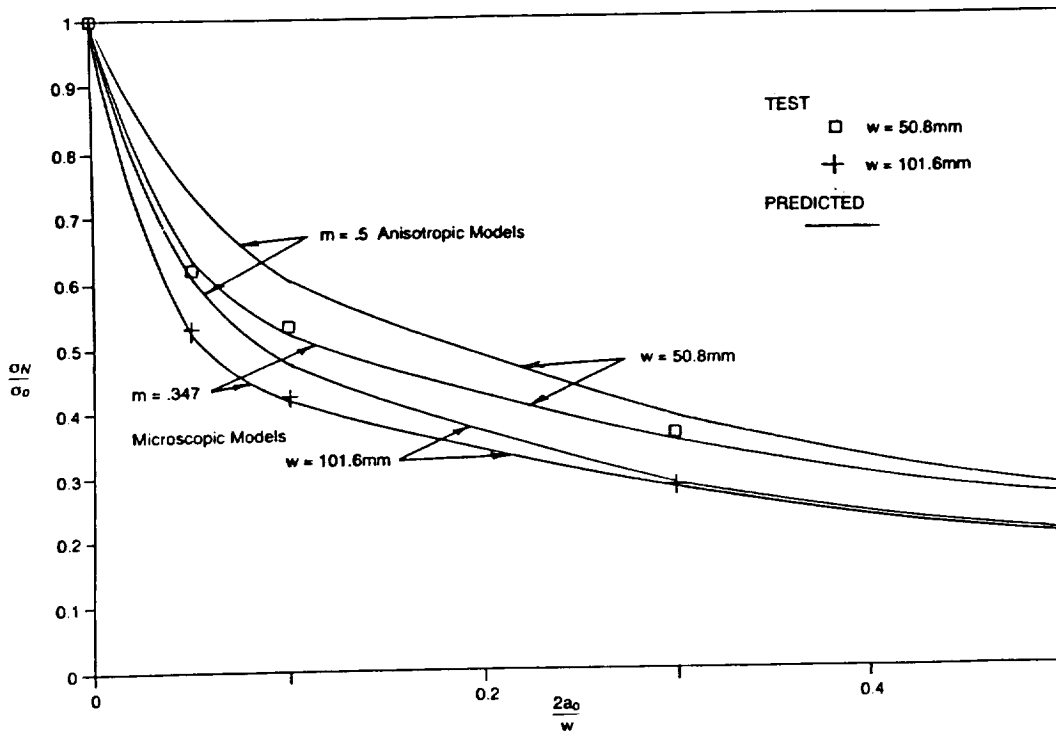


Figure 23. Comparison Of Analytical Results Between Anisotropic And New Approximate Models B/AI ($\pm 45/0_2$)_s

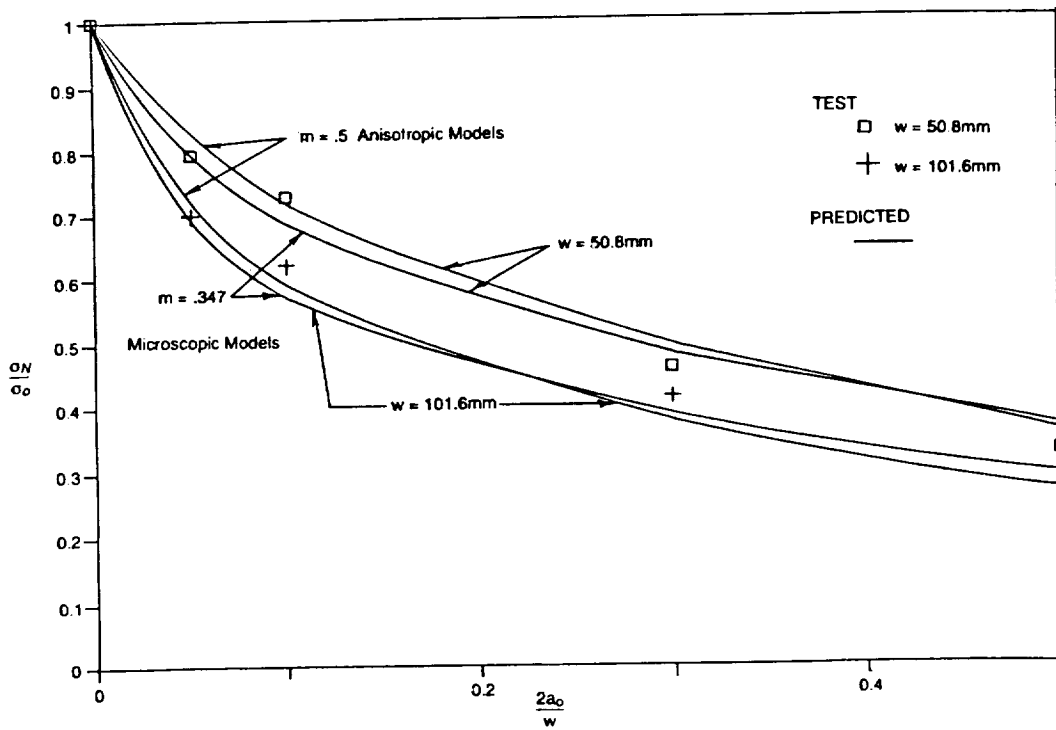


Figure 24. Comparison Of Analytical Results Between Anisotropic And New Approximate Models B/AI (0/±45)_s